Characteristics and applications of two-dimensional light scattering by cylindrical tubes based on ray tracing

Zhihong You,[1] Daya Jiang,[1] Jakob Stamnes,[3] Jianjun Chen,[1,2] and Jinghua Xiao[1,2,*]

[1]School of Science, Beijing University of Posts and Telecommunications, Beijing 100876, China

[2]State Key Laboratory of Information Photonics and Optical Communications, Beijing University of Posts and Telecommunications, Beijing 100876, China

[3]Faculty of Mathematics and Natural Sciences, University of Bergen, Bergen N-5020, Norway

*Corresponding author: jhxiao@bupt.edu.cn

Received 21 August 2012; revised 12 October 2012; accepted 15 October 2012; posted 15 October 2012 (Doc. ID 174506); published 5 December 2012

The intensity distribution of light scattered by a capillary tube filled with a liquid is studied using geometrical optics or ray tracing. Several intensity step points are found in the scattering pattern due to contributions from different geometrical rays. The scattering angles of these intensity step points vary with the capillary parameters, i.e., with the inner and outer radii of the capillary wall and the refractive indices of the liquid and the wall material. The relations between the scattering angles of the step points and the capillary parameters are analyzed using the reflection law and Snell's law. A method is developed to determine the capillary parameters from measurements of the scattering angles of the step points. An experiment is designed to provide measured data from which the capillary parameters can be obtained by the proposed method. It is shown that this method provides capillary parameters of high precision.

OCIS codes: 120.0120, 120.5820, 290.0290, 290.3030.

1. Introduction

Two-dimensional scattering of light by concentric, cylindrical structures is of great significance in quantum mechanics, optics, and radio physics. Previous researchers provided many approaches to analyze the scattering of waves by cylinders, such as the wave-equation-based Debye series expansion [1–3], the semianalytical method using multipole expansion techniques [4–7], the numerical moment method [8,9], and the Green function-based Born approximation theory [10–12]. Scattering of light from a capillary tube filled with a liquid is a typical situation of scattering by a concentric cylindrical structure. By analyzing the intensity distribution of the scattered light, one can obtain the capillary parameters, including the refractive index of the liquid [13–18]. Thus, by measuring the fringe spacing of the scattered light, one can determine the outer and inner radii of the capillary wall, and by comparing the measured fringe pattern with that obtained in simulations for different values of the refractive index of the liquid, one can determine the latter as the refractive index that provides the best agreement between the measured and simulated fringe patterns. Most of these methods are based on analyzing interference patterns, and involve complicated calculations and a lot of data processing that must be applied to the interference patterns obtained in the experiment.

In this paper, geometrical optics or ray tracing is used to analyze the intensity distribution of light scattered by a capillary tube filled with a liquid.

1559-128X/12/358341-09$15.00/0

Thus, ray tracing is used to simulate the intensity distribution of the scattered light. Several intensity step points are found to be present in the scattering pattern, and the positions of these step points vary with the capillary parameters. A simple method is developed to determine the capillary parameters, including the refractive index of the liquid, from measurements of the scattering angles of these step points. To test the validity of this method, we conducted an experiment, from which the refractive index obtained was found to deviate less than 0.5% from that measured with an Abbe refractometer. The range of capillary parameters to which the method can be applied is also discussed. Since the analysis is based on geometrical ray theory, it has a straightforward physical interpretation.

The rest of the paper is organized as follows. In Section 2, the intensity distribution of the scattered light is analyzed using geometrical ray tracing, and compared with that obtained experimentally. A method to determine the capillary parameters is presented in Section 3. In Section 4, we present results of an experiment to measure the scattered intensity distribution, from which the capillary parameters, including the liquid's refractive index, can be obtained. Finally, in Section 5, we draw our conclusions.

2. Analyzing the Intensity Distribution of the Scattered Light Using Ray Tracing

Ray tracing can be used to calculate the paths of geometrical rays by using the reflection law and Snell's law. By tracing the paths of geometrical rays that emerge in a given observation direction and adding their intensities, one can obtain the intensity of the scattered light provided interference effects can be neglected. While the path of a ray follows from repeated application of the reflection law and Snell's law [19] at the various interfaces it traverses, the intensity of each ray follows from Fresnel's equations, which give the reflectance and transmittance at each interface [20].

A. Analysis of Rays

The capillary wall is made of glass, and the refractive-index difference between the wall and air or between the wall and the liquid inside the tube is assumed to be so small that it is enough to consider at most one reflection either at the outer or at the inner capillary wall. Thus, it suffices to consider the seven different rays, denoted by ray number 1 through ray number 7 in Fig. 1.

Because of symmetry, it suffices to consider incident rays in the upper half of Fig. 1, where the angle of incidence θ is defined as the angle between the incident ray and the normal to the outer capillary wall. The angle of deviation β_k for ray number k is defined as the angle from the direction of the incident ray to the direction of the emergent ray number k with positive sign in the clockwise sense. Further, r and R are the inner and outer radii, respectively, of the capillary tube, and n and n_0 are the refractive indices

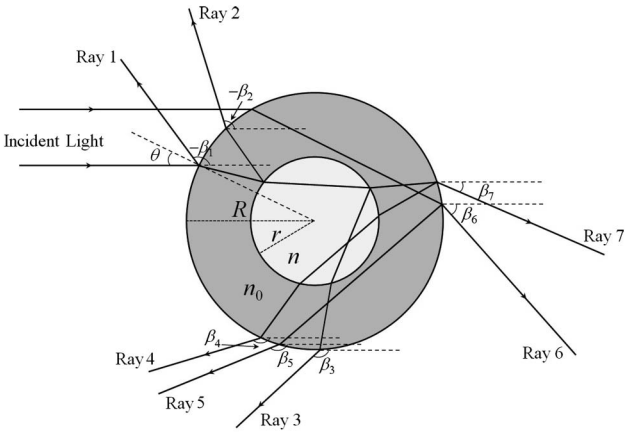

Fig. 1. Ray paths of seven different rays.

of the liquid inside the tube and the capillary wall material, respectively.

Using the reflection law and Snell's law and the geometry in Fig. 1, we find that the angles of deviation β_k $(k = 1, 2, \ldots, 7)$ are given by

$$\beta_1 = 2\theta - \pi\left[0 \le \theta \le \frac{\pi}{2}\right], \tag{1}$$

$$\beta_2 = 2\theta - 2\arcsin\frac{\sin\theta}{n_0} + 2\arcsin\frac{R\sin\theta}{rn_0} - \pi\left[0 \le \theta \le \arcsin\frac{rn_0}{R}\right], \tag{2}$$

$$\beta_3 = 2\theta - 2\arcsin\frac{\sin\theta}{n_0} + 2\arcsin\frac{R\sin\theta}{rn_0} - 4\arcsin\frac{R\sin\theta}{rn} + \pi\left[0 \le \theta \le \arcsin\frac{rn_0}{R}\right], \tag{3}$$

$$\beta_4 = 2\theta - 4\arcsin\frac{\sin\theta}{n_0} + 4\arcsin\frac{R\sin\theta}{rn_0} - 4\arcsin\frac{R\sin\theta}{rn} + \pi\left[0 \le \theta \le \arcsin\frac{rn_0}{R}\right], \tag{4}$$

$$\beta_5 = 2\theta - 4\arcsin\frac{\sin\theta}{n_0} + \pi\left[\arcsin\frac{rn_0}{R} \le \theta \le \frac{\pi}{2}\right], \tag{5}$$

$$\beta_6 = 2\left[\theta - \arcsin\frac{\sin\theta}{n_0}\right]\left[\arcsin\frac{rn_0}{R} \le \theta \le \frac{\pi}{2}\right], \tag{6}$$

$$\beta_7 = 2\left[\theta - \arcsin\frac{\sin\theta}{n_0} + \arcsin\frac{R\sin\theta}{rn_0} - \arcsin\frac{R\sin\theta}{rn}\right]\left[0 \le \theta \le \arcsin\frac{rn_0}{R}\right]. \tag{7}$$

In Eqs. (3), (4) and (7), the maximum angle of incidence $\arcsin(rn_0/R)$ is obtained only for the case in which $n > n_0$. When $n < n_0$ and the angle of incidence is larger than $\arcsin(rn/R)$, total internal reflection occurs at the interface between the capillary wall and the liquid inside the tube, making ray numbers 3, 4, and 7 disappear; thus the maximum angle of incidence is $\arcsin(rn/R)$. By taking into account the reflectance and transmittance at each interface of the capillary tube, one obtains the intensity associated with each of the seven rays.

For different angles of incidence θ in Fig. 1 and Eqs. (1)–(7), several among the seven rays may have the same deviation angle, and the total intensity then follows by adding the intensities of the contributing rays. Since the coherence length of He–Ne laser light is much larger than the difference in path length between different contributing rays, interference fringes will be present on the screen with a fringe spacing of the order of $\lambda/\Delta\beta$, where $\lambda = 0.633 \times 10^{-6}$ m is the light wavelength and $\Delta\beta = 0.013$ rad is the angular width subtended by the tube at the screen. Thus, the fringe spacing is of the order of 0.005 cm, which is too small to be observed. Note that our aim is not to determine the precise intensity distribution of the scattered light, but rather the scattering angles of the intensity step points. Thus, geometrical optics can be used to explain the experimental phenomena.

B. Intensity Distribution

Let the intensity of the incident light be $I_0(\theta)$, where θ is the angle of incidence. Then the intensity of the emerging light ray number k $(k = 1, 2, \ldots, 7)$ in the direction β_k is $I(\beta_k)$, given by

$$I(\beta_k) = S(\theta, \beta_k) I_0(\theta), \tag{8}$$

where the scattering factor $S(\theta, \beta_k)$ is the product of the reflectances and transmittances encountered by ray number k at the various interfaces. As an example, we consider $S(\theta, \beta_2)$ for ray number 2. As indicated in Fig. 1, ray number 2 undergoes refraction at the outer capillary wall at an angle of incidence θ and a corresponding angle of refraction θ', reflection at the inner capillary wall at an angle of incidence $\theta_{2,1}$ and a corresponding angle of refraction $\theta'_{2,1}$, and another refraction at the outer capillary wall at an angle of incidence $\theta_{2,2}$ and a corresponding angle of refraction $\theta'_{2,2}$. These angles follow by repeated application of the reflection law and Snell's law. The scattering factor $S(\theta, \beta_2)$ is given by the product [21]

$$S(\theta, \beta_2) = T(\theta) R(\theta_{2,1}) T(\theta_{2,2}) \left(\frac{\cos\theta}{|d\beta_2/d\theta|} \right)^{1/2}, \tag{9}$$

where the factor of $[\cos(\theta)/|d\beta_2/d\theta|]^{1/2}$ is due to the angular divergence of the light, and $T(\theta)$, $R(\theta_{2,1})$, and $T(\theta_{2,2})$ are, respectively, the transmittance associated with the refraction from air at the outer capillary wall, the reflectance associated with the reflection at the inner capillary wall, and the transmittance associated with the refraction into air at the outer capillary wall. Let the incident ray be s polarized, implying that its electric field points along the cylinder axis. Then the reflectance $R(\gamma)$ and transmittance $T(\gamma)$ are given by

$$R(\gamma) = \left[\frac{\sin(\gamma - \gamma')}{\sin(\gamma + \gamma')} \right]^2, \tag{10}$$

$$T(\gamma) = 1 - R(\gamma), \tag{11}$$

where γ stands for θ, $\theta_{2,1}$, or $\theta_{2,2}$, and γ' stands for θ', $\theta'_{2,1}$, or $\theta'_{2,2}$. The scattering factors for the other rays can be obtained in a similar manner.

As mentioned above, for different angles of incidence θ in Fig. 1 and Eqs. (1)–(7), several among the seven rays may have the same deviation angle β, and the total intensity then follows by adding the intensities of the contributing rays, i.e.,

$$I(\beta) = \sum_{i=1}^{7} S(\theta_i, \beta) I_0(\theta_i), \tag{12}$$

where the angle of incidence θ_i for each of the seven rays is chosen such that the seven rays have the same deviation angle β. Note that for a certain number ray, different incident rays may correspond to a same derivation angle; thus θ_i may not be unique, and the intensities of all these rays should be considered in order to obtain $I(\beta)$.

C. Simulated and Experimental Results

As an example, we calculated the scattered light intensity distributions for different angular regions for two capillary tubes, denoted by tube 1 and tube 2. The results are shown in Fig. 2. The parameters for tube 1 were $r/R = 0.5229$, $n_0 = 1.4710$, and $n = 1.4058$, and for tube 2 they were $r/R = 0.5192$, $n_0 = 1.4710$, and $n = 1.5278$. For tube 1 with $n < n_0$, the intensities of ray numbers 1, 2, 3, and 4 were small enough to be ignored, and for tube 2 with $n > n_0$, ray numbers 1, 2, and 3 could be ignored.

An experiment was designed to observe the intensity distribution of the scattered light in the entire angular range. To that end, a capillary tube filled with a liquid was placed perpendicularly in the center of a bowl-shaped screen made of paper, as shown in Fig. 3. A hole was made in the screen to let the incident light pass through it and reach the capillary tube. When an He–Ne laser beam (with wavelength 632.8 nm) polarized along the axis of the capillary tube was normally incident upon it, the pattern of the scattered light appeared on the screen, which was imaged by a camera above it. The experimental scattering patterns for tube 1 and tube 2 are shown in Figs. 4(a) and 4(b), respectively, and the corresponding simulation results are shown in Figs. 4(c) and 4(d), respectively.

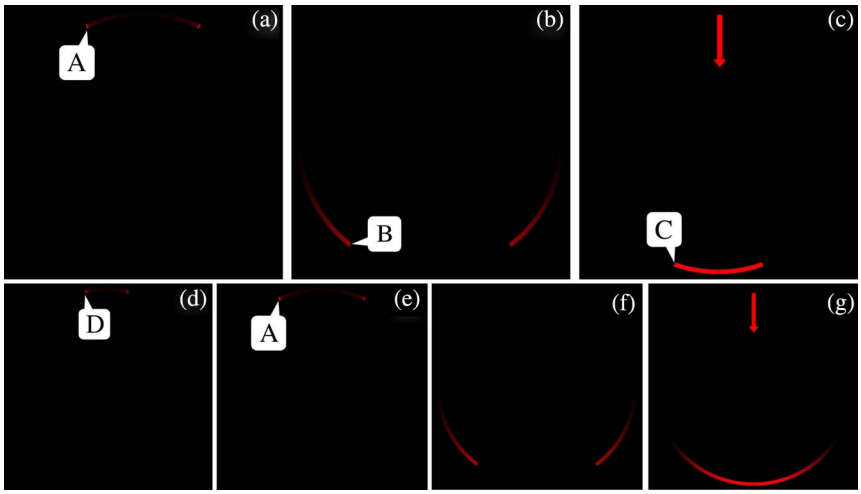

Fig. 2. (Color online) Intensity distributions of different angular parts of the scattered light for tube 1 and tube 2. (a)–(c) correspond to ray numbers 5–7, respectively, for tube 1, and (d)–(g) correspond to ray numbers 4–7, respectively, for tube 2. The arrow represents the direction of the incident light.

The simulations are seen to be in good agreement with the experimental results, except for the bright spots at the bottom of the experimental patterns in Figs. 4(a) and 4(b), which were due to unscattered laser light. Another difference between simulation and experiment is that in the simulated intensity pattern in Fig. 4(d) there is an intensity step point at point B at a scattering angle of about 30°, whereas there is no such intensity step point in the experimental pattern in Fig. 4(b). The reason for this difference is mainly caused by the coherence of the incident laser light. When $n > n_0$, rays 6 and 7 have comparable intensities at point B, where they interfere to produce fringes, which are difficult to see in Fig. 4(b), but visible by close inspection. These closely spaced interference fringes disguise the intensity step point that would have been visible in their absence. In the simulated intensity pattern in Fig. 4(d), one can see this intensity step point because interference is not accounted for in the simulation. When $n < n_0$, there were three intensity step points in the pattern, denoted by A, B, and C, respectively, as shown in Fig. 4(a). When $n > n_0$, another intensity step point appeared near A, denoted by D, and the intensity step points B and C were no longer present, as shown in Fig. 4(b). Comparisons of Figs. 2 and 4 showed that the intensity step points A, B, and D corresponded to the minimum deviation angles of ray numbers 5, 6, and 4, respectively, and that point C corresponded to the maximum deviation angle of ray number 7. The relations between the scattering angles of these intensity step points and the capillary parameters are analyzed in Section 3.

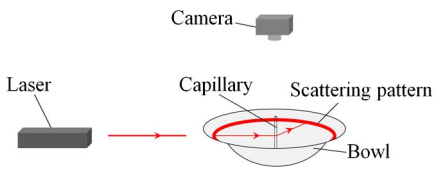

Fig. 3. (Color online) Experimental setup to observe the intensity distribution of the scattered light. The diameter of the observing screen is about 15 cm.

3. Relations Between Scattering Angles of Intensity Step Points and Capillary Parameters

As mentioned above, the scattering angles of the intensity step points vary with the capillary parameters. Therefore, measurements of the scattering angles of the intensity step points can be used to determine the capillary parameters. To that end, relations between the scattering angles of the intensity step points and the capillary parameters must be established.

A. Relation Between Point A and n_0

The scattering angle of intensity step point A corresponds to the minimum deviation angle of ray

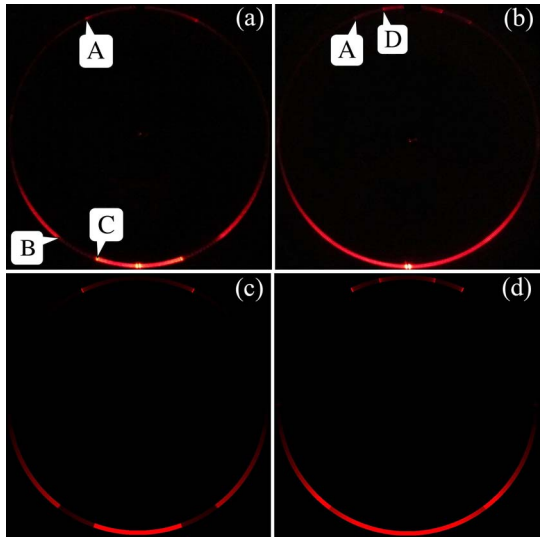

Fig. 4. (Color online) Experimental intensity patterns for (a) tube 1 and (b) tube 2. Simulated intensity patterns for (c) tube 1 and (d) tube 2.

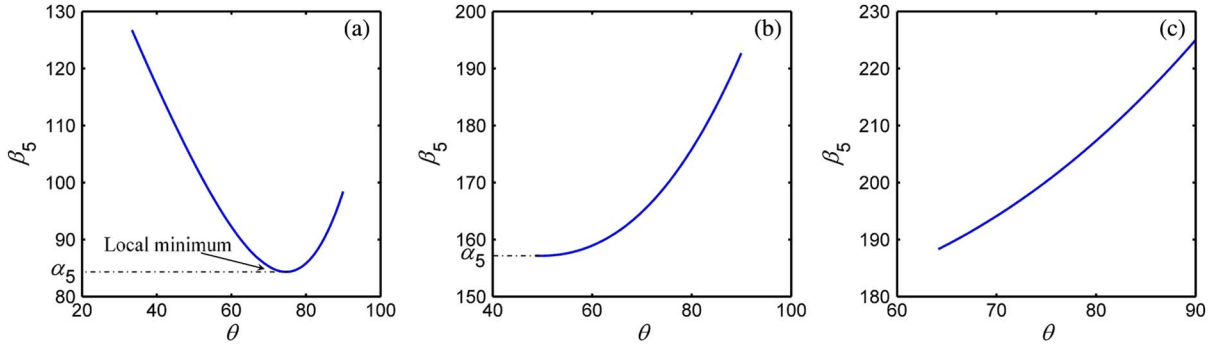

Fig. 5. (Color online) Plots of β_5 versus θ for different values of n_0, for $r/R = 0.5$, and for refractive indices of the capillary material of (a) $n_0 = 1.10$, (b) $n_0 = 1.51$, and (c) $n_0 = 1.80$.

number 5, denoted by α_5. Plots of β_5 versus θ for different values of n_0 are shown in Fig. 5 based on Eq. (5), and the corresponding simulated intensity distributions of the scattered light are shown in Fig. 6. Figures 5 and 6 show that intensity step point A exists if and only if β_5 has a local minimum. Figure 5(b) shows a limiting case.

As we can see in Eq. (5), $|d\beta/d\theta|$ is inversely proportional to the intensity of scattered light at a certain angle. Thus, a small slope of the β versus θ curve means a small divergence or angular spread, and thus a high intensity. Since ray number 5 contains reflected light, it has low intensity in general. Only at the scattering angle corresponding to a local minimum of the angular spread can the contribution of ray number 5 be observed in the scattering pattern. At other scattering angles, ray number 5 is dark, implying that intensity step point A is absent. Thus, the condition for the existence of intensity step point A is that β_5 has a local minimum.

Differentiating β_5 in Eq. (5) with respect to θ, and setting the derivative equal to zero, we obtain the angle of incidence, denoted by θ_{5m}, corresponding to the minimum of β_5:

$$\theta_{5m} = \arcsin\left(\frac{4 - n_0^2}{3}\right)^{1/2}. \tag{13}$$

The condition for the existence of a minimum of β_5 is that θ_{5m} lies in the range of angles of incidence associated with ray number 5, i.e., [cf. Eq. (5)],

$$\arcsin\frac{rn_0}{R} < \theta_{5m} < \frac{\pi}{2}. \tag{14}$$

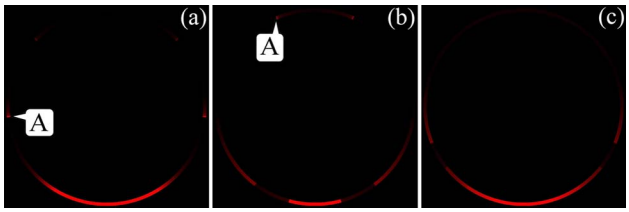

Fig. 6. (Color online) Intensity distributions of the scattered light for different values of n_0. The capillary parameters are $n = 1.4$, $r/R = 0.5$, and (a) $n_0 = 1.10$, (b) $n_0 = 1.51$, and (c) $n_0 = 1.80$.

Substituting from Eq. (13) into Eq. (14), we find that the condition for the existence of point A is

$$1 < n_0 < \left(\frac{4}{1 + 3r^2/R^2}\right)^{1/2}. \tag{15}$$

Substituting from Eq. (13) into Eq. (5), we obtain the scattering angle of point A:

$$\alpha_5 = 2\arcsin\left(\frac{4 - n_0^2}{3}\right)^{1/2} - 4\arcsin\left(\frac{4 - n_0^2}{3n_0^2}\right)^{1/2} + \pi. \tag{16}$$

From Eq. (16), we see that n_0 depends only on α_5, and Fig. 7 shows the relation between α_5 and n_0. We conclude that by measuring the scattering angle of the intensity step point A, we can determine n_0 by using the plot in Fig. 7, where the range of n_0 is given in Eq. (15).

B. Relation Between Point B and r/R

The scattering angle of intensity step point B corresponds to the minimum deviation angle of ray number 6, denoted by α_6. From Eq. (6), it follows that β_6 increases monotonically with θ, so that α_6 can be obtained by inserting the minimum value of θ, given by $\arcsin(rn_0/R)$, into Eq. (6):

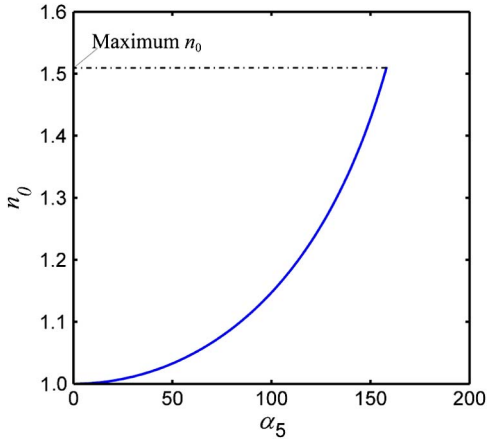

Fig. 7. (Color online) Relation between α_5 and n_0 for $r/R = 0.5$.

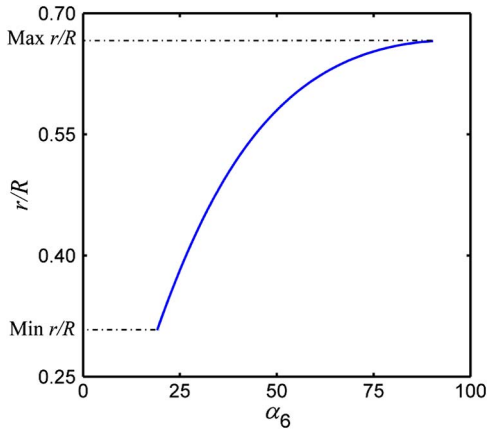

Fig. 8. (Color online) Relation between α_6 and r/R. The refractive indices of the capillary and liquid are $n_0 = 1.5$ and $n = 1.3$, respectively.

$$\alpha_6 = 2 \arcsin \frac{rn_0}{R} - 2 \arcsin \frac{r}{R}. \tag{17}$$

Once n_0 has been determined from Fig. 7, r/R depends only on α_6, as illustrated in Fig. 8.

To determine the minimum and maximum values or lower and upper bounds for r/R in Fig. 8, we first take a look at the simulated intensity distributions for different ratios r/R in Fig. 9, from which it follows that there is a minimum value for r/R. For r/R values smaller than the minimum value, ray number 7 will diverge and disguise intensity step point B, as is evident from comparing the bottom portions of Figs. 9(a) and 9(b). The condition for nondivergence of ray number 7, which will be obtained below, is

$$\frac{1}{r/R - r/(Rn_0) + 1/n_0} < n, \tag{18}$$

from which it follows that the minimum value for r/R is $(n_0 - n)/(n_0 n - n)$.

According to Eq. (6), the lower bound for the angle of incidence for ray number 6 is $\arcsin(rn_0/R)$. When r/R increases to $1/n_0$, the lower bound for the angle of incidence for ray number 6 approaches $\pi/2$ and ray number 6 disappears, as illustrated in Fig. 9(d), where r/R has the value 0.7, which is larger than $1/n_0 = 0.67$. Thus, the upper bound for r/R is $1/n_0$, implying that we can determine r/R from Fig. 8 in the range from $(n_0 - n)/(n_0 n - n)$ to $1/n_0$.

C. Relations Between n and Intensity Step Points C, D, and E

The scattering angles of intensity step points C and D correspond to respectively the maximum value of β_7, denoted by α_7, and the minimum value of β_4, denoted α_4. By simulating the intensity distributions for the scattered light for different values of the refractive index n of the liquid, we found intensity step point C to exist when $n < n_0$ [Fig. 10(a)] but to disappear when $n > n_0$, in which case intensity step point D emerged [Fig. 10(b)]. As n continued to increase, point D disappeared, whereas another intensity step point, denoted by E, appeared [Fig. 10(c)]. It corresponds to the minimum deviation angle of ray number 3, denoted by α_3. Simulations indicate that the scattering angles of intensity step points C, D, and E vary with the refractive index n of the liquid, which therefore may be determined from measurements of these scattering angles.

First, we analyze the ranges of n that can be determined from measurements of the scattering angles of intensity step points C, D, and E. Plots of β_4 versus θ for different values of n are shown in Fig. 11, and the corresponding simulated intensity distributions for ray number 4 are shown in Fig. 12. Intensity step point D exists if and only if β_4 has a local minimum, as illustrated in Figs. 11(b) and 12(b). Otherwise ray

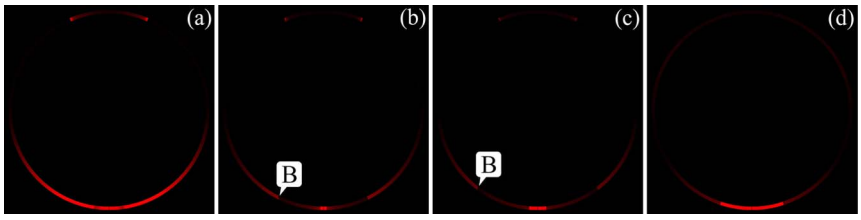

Fig. 9. (Color online) Intensity distributions of the scattered light for different values of r/R. The parameters are $n_0 = 1.5$, $n = 1.3$, and (a) $r/R = 0.15$, (b) $r/R = 0.40$, (c) $r/R = 0.5$, and (d) $r/R = 0.70$.

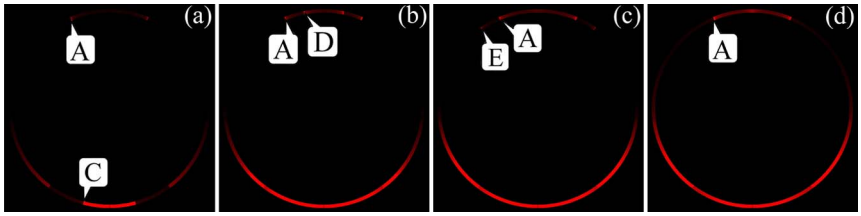

Fig. 10. (Color online) Intensity distributions of light scattered by capillary tubes filled with different liquids. The parameters are $r/R = 0.5$, $n_0 = 1.5$, and (a) $n = 1.40$, (b) $n = 1.55$, (c) $n = 1.80$, and (d) $n = 2.50$.

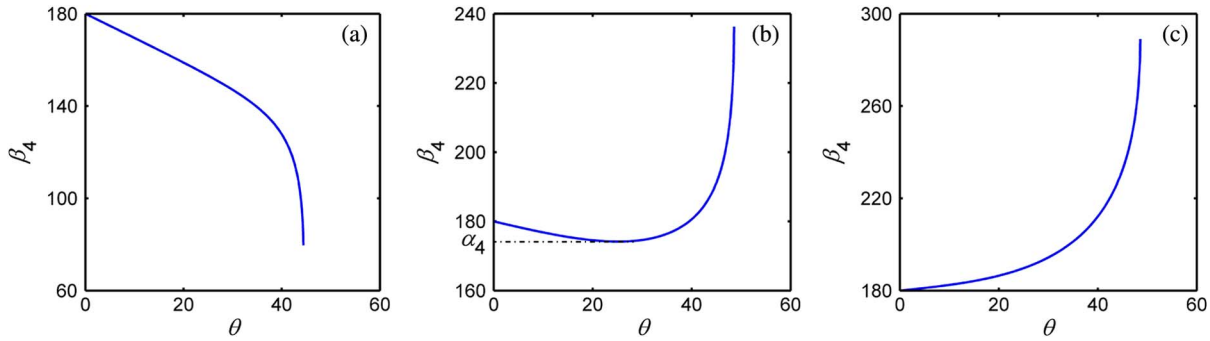

Fig. 11. (Color online) Plots of β_4 versus θ for different values of n. The parameters are $r/R = 0.5$, $n_0 = 1.5$, and (a) $n = 1.4$, (b) $n = 1.6$, and (c) $n = 1.8$.

4 diverges and intensity step point D disappears, as shown in Figs. 11(a) and 12(a) and also in Figs. 11(c) and 12(c). Thus, the condition for existence of intensity step point D is that β_4 has a local minimum, implying that the slope of β_4 is negative for values of θ smaller than θ_{4m}, which corresponds to the minimum value of β_4, whereas the slope of β_4 is positive for values of θ larger than θ_{4m}. Thus

$$\frac{d\beta_4}{d\theta} < 0 \quad \text{when } \theta \text{ has its minimum value,} \tag{19}$$

and

$$\frac{d\beta_4}{d\theta} > 0 \quad \text{when } \theta \text{ has its maximum value.} \tag{20}$$

When $n < n_0$, the minimum and maximum angles of incidence of ray number 4 are 0 and $\arcsin(rn/R)$, respectively [see Eq. (4) and the first two sentences after Eq. (7)]. Substituting this maximum value of θ into the derivative of Eq. (4) with respect to θ, we obtain

$$\frac{d\beta_4}{d\theta} = -\infty \quad \text{for } \theta = \arcsin\left(\frac{rn}{R}\right). \tag{21}$$

Since Eq. (21) is in contradiction with relation (20), point D cannot exist when $n < n_0$. When $n > n_0$, the minimum and maximum incident angles of ray 4 are 0 and $\arcsin(rn_0/R)$. Substituting these minimum and maximum values of θ into the derivative of Eq. (4) with respect to θ, we obtain from relations (19) and (20)

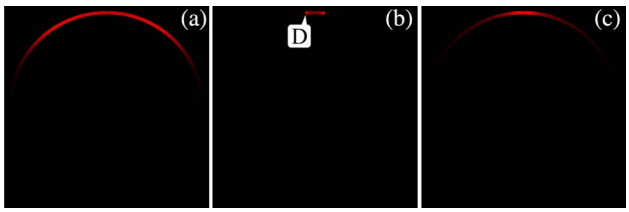

Fig. 12. (Color online) Intensity distributions of scattered light for ray number 4. The parameters are $r/R = 0.5$, $n_0 = 1.5$, and (a) $n = 1.4$, (b) $n = 1.6$, and (c) $n = 1.8$.

$$\frac{d\beta_4}{d\theta} = 2\left(1 - \frac{2}{n_0} + \frac{2R}{rn_0} - \frac{2R}{rn}\right) < 0 \quad \text{for } \theta = 0, \tag{22}$$

$$\frac{d\beta_4}{d\theta} = +\infty \geq 0 \quad \text{for } \theta = \arcsin\left(\frac{rn_0}{R}\right). \tag{23}$$

Since relation (23) is always satisfied, the range of n that can be determined from measurements of the scattering angle of point D follows from relation (22):

$$n_0 < n < \frac{1}{r/(2R) - r/(Rn_0) + 1/n_0}. \tag{24}$$

The ranges of n that can be determined from measurements of the scattering angles of intensity step points C and E can be obtained by using the same procedure:

$$\frac{1}{r/R - r/(Rn_0) + 1/n_0} < n < n_0 \quad \text{(point C)} \tag{25}$$

and

$$n_0 < n < \frac{2}{r/R - r/(Rn_0) + 1/n_0} \quad \text{(point E).} \tag{26}$$

Analytic expressions of α_3, α_4, and α_7 are hard to obtain. However, the relations between each of these quantities and n can be obtained numerically from Eqs. (3), (4), and (7), respectively, as shown in Fig. 13 for four different values of n ($n = n_1$, $n = n_2$, $n = n_3$, and $n = n_4$), given by $n_1 = 1/[r/R - r/(Rn_0) + 1/n_0]$, $n_2 = n_0$, $n_3 = 1/[r/(2R) - r/(Rn_0) + 1/n_0]$, and $n_4 = 2/[r/R - r/(Rn_0) + 1/n_0]$, for $n_0 = 1.471$ and $r/R = 0.5$. When $n_2 < n < n_3$, one cannot determine n from measurements of the scattering angle of intensity step point E, because then point E is disguised by background light and thus invisible, as shown in Fig. 10(b). In conclusion, n can be determined from measurements of the scattering angles of intensity step point C when $n_1 < n < n_2$, intensity step point D when $n_2 < n < n_3$, and intensity step point E when $n_3 < n < n_4$. For example, with $n_0 = 1.5$ and $r/R = 0.5$, one can determine the refractive

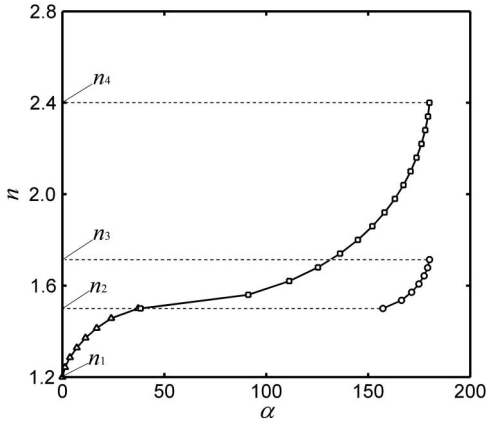

Fig. 13. Relations between n and the scattering angles of points C (triangle), D (circle), and E (square). The refractive index and the radius ratio of the capillary tube are $n_0 = 1.5$ and $r/R = 0.5$, respectively.

indices of liquids in the range from $n = 1.2$ to $n = 2.4$, which covers most liquids.

D. Summary of the Method

For a brief overview of the method, the results of the previous analyses are listed in Table 1, where a complete method is presented for determining the capillary parameters from measurements of the scattering angles of the intensity step points.

4. Experimental Results

To test our method, an experiment was designed to determine the capillary parameters from measurements of the scattering angles of the intensity step points. Figure 14 shows the experimental apparatus, which was made by modifying a spectrometer.

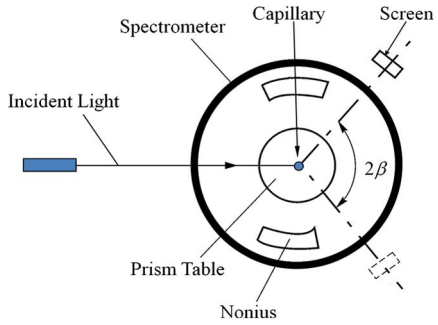

Fig. 14. (Color online) Experimental setup to measure the scattering angles of intensity step points.

A capillary tube is placed on the objective stage parallel to the main axis of the spectrometer. An observing screen with a scale is fixed on the spectrometer arm, which can move circularly around the main axis of the spectrometer. By rotating the screen, one can observe the intensity distribution of the scattered light at any angle, and thus measure the scattering angles of the intensity step points with an accuracy of 1′. The measured angles of the intensity step points for tube 1 and tube 2 are shown in Table 2.

By using the measured angles in Table 2, one can obtain the capillary parameters, as shown in Table 3, where the differences are seen to be smaller than 0.5% between our results and those obtained with an Abbe refractometer, which is an instrument based on the principle of total internal reflection. When light from different directions is incident on a sample in an Abbe refractometer, the incident light will be totally reflected at angles of incidence equal to or larger than the critical angle. Thus, by measuring the critical angle of deviation at which total reflection

Table 1. Brief List of the Method

Parameter	Step Point	Range	Premised	Relation
n_0	A	$1 \sim [4/(1+3r^2/R^2)]^{1/2}$	None	Fig. 7
r/R	B	$(n_0-n)/(n_0 n-n) \sim 1/n_0$	n_0	Fig. 8
n	C	$n_1 \sim n_2$	n_0, r/R	Fig. 13 (triangle)
n	D	$n_2 \sim n_3$	n_0, r/R	Fig. 13 (circle)
n	E	$n_3 \sim n_4$	n_0, r/R	Fig. 13 (square)

Table 2. Measured Scattering Angles of Intensity Step Points for Capillaries with Different Liquids Inside[a]

Liquid	Point A	Point B	Point C	Point D
Simethicone	154°55′	37°41′	19°9′	
Phenethyl alcohol	154°44′			167°3′

[a]The capillary with phenethyl alcohol inside is of radius ratio 0.5192.

Table 3. Results Obtained by Using Our Method and Other Precise Methods[a]

Liquid	n_0	n_0'	Error	n	n'	Error	r/R	r'/R'	Error
Simethicone	1.4762	1.4710	0.35%	1.4063	1.4058	0.04%	0.5203	0.5229	0.50%
Phenethyl alcohol	1.4740	1.4710	0.2%	1.5260	1.5278	0.12%			

[a]n_0, r/R, and n are measured by using our method. n_0' and n' are obtained from an abbe refractometer, and r'/R' is obtained from a JCD3 50 mm reading microscope.

starts, the refractive index of the sample can be determined from Snell's law [22].

The main errors in the experiment are due to the wave nature of light and the asymmetry of the capillary. The wave nature of light is responsible for distributing each intensity step point in the experiment in a small angular range instead of a single point, which results in an uncertainty in the measurement of the scattering angle of each intensity step point. A capillary tube with a larger size would reduce the influence from the wave nature of light, and make the results more precise. The asymmetry of the capillary tube is unavoidable when the objective is to measure its parameters. But if one just wants to measure the refractive index of a liquid, then one could choose a more symmetrical capillary by rotating it around its axis to check whether the rotation results in movements of the intensity step points. The less the step-point movements, the more symmetrical the capillary.

5. Conclusion

The intensity distributions of light scattered by a capillary tube filled with a liquid were simulated and obtained experimentally, and the simulations were found to be in good agreement with the experimental results. A new, accurate method was developed to determine the capillary parameters, including the refractive index of the liquid, by using measured values of the scattering angles of various intensity step points. Since the method is based on geometrical ray theory, without consideration of interference effects, it has a straightforward physical interpretation. Only the scattering angles of certain intensity step points are analyzed theoretically and obtained experimentally, making the method simple. This method can be used to measure the refractive index of a poisonous or flammable liquid because the liquid is encapsulated in the capillary tube, which is not possible when using traditional methods. We can also use this method to measure other parameters of the liquid if they are related to its refractive index. As the container of the liquid is a long and thin tube, the liquid inside it can be easily renewed by feeding a new liquid from one side of the tube and removing the old liquid from the other side, implying that this method can dynamically measure the liquid's refractive index and related parameters.

This work was supported by the National Basic Research Program of China (Grant No. 2010CB923200). The authors would like to thank Doctor Hujiang Yang for beneficial suggestions.

References

1. J. A. Lock and C. L. Adler, "Debye-series analysis of the first-order rainbow produced in scattering of a diagonally incident plane wave by a circular cylinder," J. Opt. Soc. Am. A **14**, 1316–1328 (1997).
2. J. Shen and H. Wang, "Calculation of Debye series expansion of light scattering," Appl. Opt. **49**, 2422–2428 (2010).
3. R. Li, X. Han, H. Jiang, and K. F. Ren, "Debye series of normally incident plane-wave scattering by an infinite multilayered cylinder," Appl. Opt. **45**, 6255–6262 (2006).
4. M. Yokota and M. Sesay, "Two-dimensional scattering of a plane wave from a periodic array of dielectric cylinders with arbitrary shape," J. Opt. Soc. Am. A **25**, 1691–1696 (2008).
5. E. Moreno, D. Erni, C. Hafner, and R. Vahldieck, "Multiple multipole method with automatic multipole setting applied to the simulation of surface plasmons in metallic nanostructures," J. Opt. Soc. Am. A **19**, 101–111 (2002).
6. H. M. Al-Rizzo and J. M. Tranquilla, "Electromagnetic wave scattering by highly elongated and geometrically composite objects of large size parameters: the generalized multipole technique," Appl. Opt. **34**, 3502–3521 (1995).
7. G. Roll, T. Kaiser, S. Lange, and G. Schweiger, "Ray interpretation of multipole fields in spherical dielectric cavities," J. Opt. Soc. Am. A **15**, 2879–2891 (1998).
8. G. Bourlier, G. Kubické, and N. Déchamps, "Fast method to compute scattering by a buried object under a randomly rough surface: PILE combined with FB-SA," J. Opt. Soc. Am. A **25**, 891–902 (2008).
9. H. Ameri, R. F. Dana, and S. Member, "Green's function analysis of electromagnetic wave propagation in photonic crystal devices using complex images technique," J. Lightwave Technol. **29**, 298–304 (2011).
10. K. Kvien, "Validity of weak-scattering models in forward two-dimensional optical scattering," Appl. Opt. **34**, 8447–8459 (1995).
11. A. Brancaccio, G. Leone, and R. Pierri, "Information content of Born scattered fields: results in the circular cylindrical case," J. Opt. Soc. Am. A **15**, 1909–1917 (1998).
12. S. Caorsi, A. Massa, and M. Pastorino, "Bistatic scattering-width computation for weakly nonlinear dielectric cylinders of arbitrary inhomogeneous cross-section shapes under transverse-magnetic wave illumination," J. Opt. Soc. Am. A **12**, 2482–2490 (1995).
13. S. Calixto, M. R. Aguilar, D. M. Hernandez, and V. P. Minkovich, "Capillary refractometer integrated in a microfluidic configuration," Appl. Opt. **47**, 843–848 (2008).
14. H. E. Ghandoor, E. Hegazi, I. Nasser, and G. M. Behery, "Measuring the refractive index of crude oil using a capillary tube interferometer," Opt. Laser Technol. **35**, 361–367 (2003).
15. H. J. Tarigan, P. Neill, C. K. Kenmore, and D. J. Bornhop, "Capillary-scale refractive index detection by interferometric backscatter," Anal. Chem. **68**, 1762–1770 (1996).
16. S. Qi, X. Yang, C. Zhang, L. Zhang, X. Wang, T. Xu, J. Tian, and G. Zhang, "Analysis of capillary interferometry for measuring refractive indices of minute samples," Appl. Opt. **43**, 530–536 (2004).
17. Z. Hou, X. Zhao, and J. Xiao, "A simple double-source model for interference of capillaries," Eur. J. Phys. **33**, 199–206 (2012).
18. A. Yang, W. Li, G. Yuan, J. Dong, and J. Zhang, "Measuring the refractive indices of liquids with a capillary tube interferometer," Appl. Opt. **45**, 7993–7998 (2006).
19. M. Born and E. Wolf, *Principles of Optics*, 7th ed. (Cambridge University, 1999), pp. 132–133.
20. M. Born and E. Wolf, *Principles of Optics*, 7th ed. (Cambridge University, 1999), pp. 40–49.
21. Y. Takano and M. Tanaka, "Phase matrix and cross sections for single scattering by circular cylinders: a comparison of ray optics and wave theory," Appl. Opt. **19**, 2781–2793 (1980).
22. Wikipedia, "Abbe refractometer," http://en.wikipedia.org/wiki/Abbe_refractometer.